A Simple Treatment for the Irreversible Optimization of the Electrical Conductivity of Poly(3,4-ethylenedioxythiophene)

Tratamiento simple para la optimización irreversible de la conductividad eléctrica de poli(3,4-etilendioxitiofeno)

Margarita Sánchez-Jiménez[1,*], Rafael S. Peres[2,3,*], Francisco Casellas[4], Carlos A. Ferreira[3], Lourdes Franco[2], Jordi Puiggalí[2,5], Francesc Estrany[1,5] and Carlos Alemán[2,5]

Abstract

Compact and porous films of poly(3,4-ethylenedioxythiophene) (PEDOT), which were prepared in aqueous and acetonitrile solutions, have been submitted to a simple thermal treatment that provokes irreversible changes in the structure and electrical conductivity. This consists of a heating-cooling cycle in which the temperature is moderately increased from 25 ºC to 70 ºC at a slow rate (1 ºC/min) and subsequently cooled to room temperature at an even slower rate (0.5 ºC/min). As a consequence, the electrical conductivity of the films prepared in water and acetonitrile irreversibly increases 864% (x8.6) and 80% (x1.8), respectively. Structural studies show that the proposed treatment provokes local re-organizations of the polymer chains and clusters, depending on the compactness of the prepared samples. In the case of films prepared in water, which are the most compact, structural re-organizations of the already formed clusters give place to the formation of large aggregates that are clearly observed on the surface. In this percolative mechanism, the interconnections among neighbouring conductive clusters embedded in such aggregates are improved leading to increased conductivity. In contrast, the improvement in the conductivity of films prepared in acetonitrile is due to the enhanced crystallinity that results from the re-arrangement of polymer molecules.

Keywords

PEDOT, conducting polymer, heat treatment, restructuring, percolation.

Resumen

La aplicación de un tratamiento térmico a películas compactas y porosas de poli(3,4-etilendioxitiofeno) (PEDOT), preparadas en soluciones acuosas y de acetonitrilo, provoca cambios irreversibles en la estructura y la conductividad eléctrica. Este tratamiento consiste en un ciclo de calentamiento-enfriamiento en el que se aumenta la temperatura de 25 °C a 70 °C lentamente (1 °C/min) y, posteriormente, se enfría a temperatura ambiente a un ritmo incluso más lento (0,5 °C/min). Como resultado, la conductividad eléctrica de las películas preparadas en agua y acetonitrilo aumenta de forma irreversible el 864% (8,6 veces) y el 80% (1,8 veces), respectivamente. Los estudios estructurales muestran que este tratamiento provoca reorganizaciones locales de las cadenas y agrupamientos de polímero, en función de la compactación de las muestras preparadas. En el caso de las películas preparadas en agua, que son las más compactas, las reorganizaciones estructurales de los grupos ya formados dan lugar a la formación de grandes agregados que se observan con claridad en la superficie. En este mecanismo de percolación, las interconexiones entre los grupos conductores vecinos embebidas en dichos agregados dan como resultado un aumento de la conductividad. Por el contrario, la mejora en la conductividad de las películas preparadas en acetonitrilo se debe a las mejoras en el grado de cristalización resultantes de la reorganización de las moléculas del polímero.

Palabras clave

PEDOT, polímero conductor, tratamiento térmico, reestructuración, percolación.

Recibido / *Received*: 2.11.2016. Aceptado / *Accepted*: 31.01.2017

[1]Departament d'Enginyeria Química, Escola Universitària d'Enginyeria Tècnica Industrial de Barcelona, Universitat Politècnica de Catalunya, Comte d'Urgell 187, 08036 Barcelona, Spain. [2]Departament d'Enginyeria Química, E. T. S. d'Enginyers Industrials, Universitat Politècnica de Catalunya, Diagonal 647, 08028, Barcelona, Spain. [3]Departamento de Engenharia de Materiais, PPGEM, Universidade Federal do Rio Grande do Sul, Av. Bento Gonçalvez, 9500, Sector 4, Prédio 74- 91501-970, Porto Alegre (RS), Brazil. [4]Departament d'Enginyeria Electrònica, Escola Universitària d'Enginyeria Tècnica Industrial de Barcelona, Universitat Politècnica de Catalunya, Comte d'Urgell 187, 08036 Barcelona, Spain. [5]Center for Research in Nano-Engineering, Universitat Politècnica de Catalunya, Campus Sud, Edifici C', C/Pasqual i Vila s/n, Barcelona E-08028, Spain. *These authors contributed equally to this work.
Autor para correspondencia / *Corresponding author*: francesc.estrany@upc.edu; carlos.aleman@upc.edu

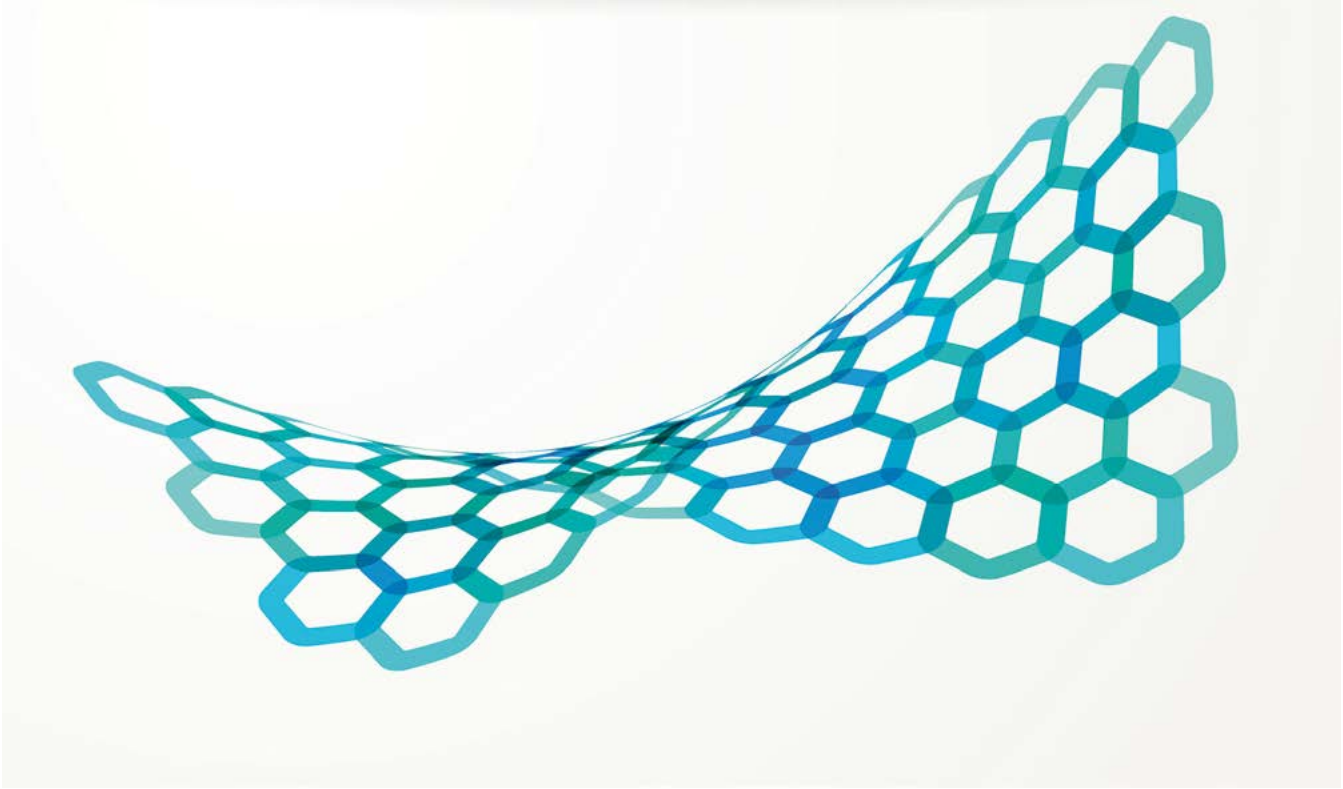

Foto: Shutterstock

Introduction

Polythiophene derivatives have been settled among the most promising CPs for optoelectronic devices (Nielsen et al 2013, Kim et al 2006). In particular, the excellent performance of poly(3-hexylthiophene) and, specially, poly(3,4-ethylenedioxythiophene (PEDOT) for optoelectronics have been recently reported (Jang et al 2009, Jang et al 2010, Dayal et al 2010, Tada 2013, Nardes et al 2012). PEDOT (Scheme 1), which exhibits low band gap (1.6-1.7 eV), high conductivity and good environmental stability (Groenendaal et al 2000, Kirchmeyer 2005, and Pettersson et al 1999), has been employed to fabricate electrochromic devices (Kumar A et al, 1998), fuel cells (Winther-Jensen et al, 2008) field emitters (Joo et al, 2005), dye-sensitized solar cells (DSSCs) (Koh et al, 2011) and organic batteries (Xuan et al, 2012 and Aradilla et al, 2014).

The optoelectronic properties of conjugated polymers as electrodes are known to be related with the morphological properties of the active material (Hoppe 2006, Schwartz 2003 and Nardes *et al*, 2008). Temperature dependent conductivity measurements are the most simple and direct way to evaluate the charge transport mechanism of CPs. Within this context, Nardes *et al* (2008) correlated the enhanced conductivity and morphological changes experienced by PEDOT doped with poly(4-styrenesulfonate) (PEDOT:PSS) that is obtained by addition of high-boiling solvents, such as sorbitol, to the aqueous dispersion used for film deposition. Results showed that PEDOT-rich 3D clusters of untreated films transform into elongated domains (*i.e.* 1D aggregates) in sorbitol-treated films, which was consistent with a change in the charge transport mechanism from 3D variable range hopping to quasi-1D variable range hopping. After the work of Nardes *et al* (2008), the variation of the conductivity with the temperature of PEDOT has been studied by different authors (Culebras *et al*, 2014; Wu *et al*, 2013; Wilson 2013, and Bubnova *et al*, 2011). On the other hand, different physical treatments have proposed in the last years to enhance the conductivity and the thermoelectric performance of PEDOT (Luo *et al*, 2013; Anatasov *et al*, 2014; Xia 2010, and Castagnola *et al*, 2014). For example, Luo *et al* (2013) enhanced the thermoelectric properties of PEDOT:PSS through post-treatments based on the addition of polar solvents or mixtures of polar solvents and ionic liquids, whereas Xia (2010) reported a similar strategy based on the addition of organic and inorganic acids. More recently, Atanasov *et al* (2014) reported that the growth temperature strongly affects the crystalline structure and electronic conductivity of PEDOT, films deposited at 150 ºC exhibiting conductivities above 1,000 S/cm. Castagnola *et al* (2014) reported that the electrochemical polymerization route affects the conductivity and morphology of PEDOT:PSS. In a very recent study Lee *et al* (2014) evidenced that sequential doping and dedoping increases the conductivity and thermoelectric behaviour of PEDOT:PSS, even though no correlation with morphological changes was provided.

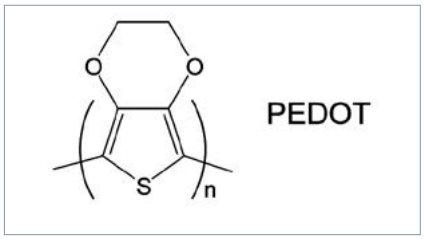

Scheme 1

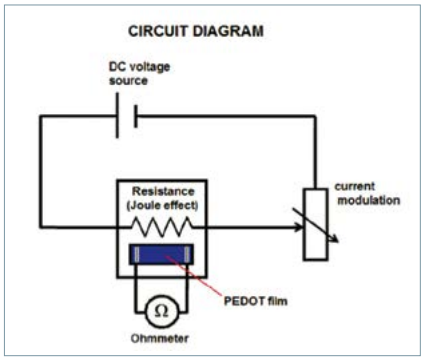

Figure 1. Schematic circuit used for heating-cooling treatment and electrical measurements.

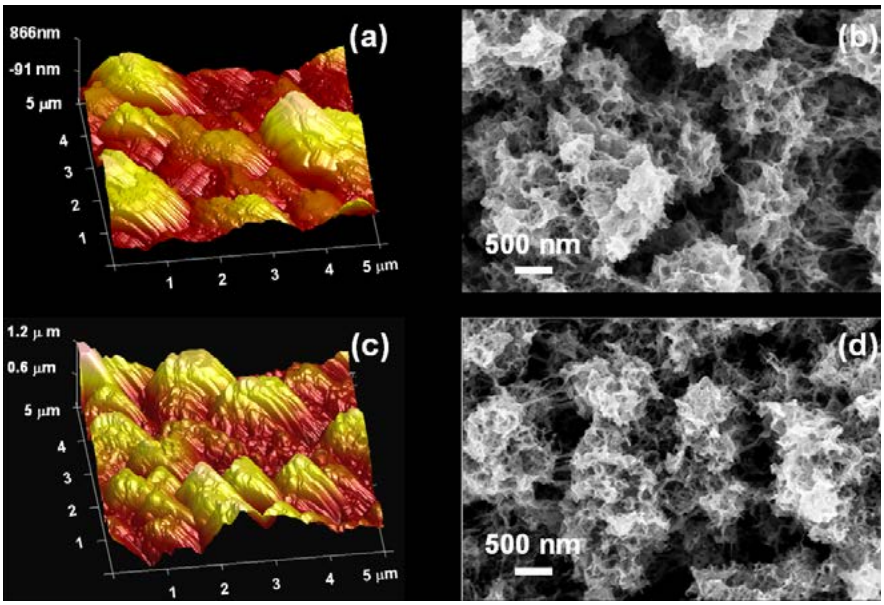

Figure 2. 3D AFM and SEM micrographs for PEDOT prepared in acetonitrile: (a,b) pristine samples; and (c,d) samples subjected to heating-cooling treatment.

In this work we propose a heating-cooling treatment to enhance the electrical performance of PEDOT doped with ClO_4^-. Furthermore, the influence of the polymerization medium has been also examined by considering films prepared in two different environments, organic (*i.e.* acetonitrile), and aqueous solutions. The study has been accompanied by morphological, topographical and structural analyses to explain the phenomena that promote the conductivity enhancement. In addition to its simplicity, the main advantages of the proposed treatment consist of both the stability of the achieved conductivity (*i.e.* changes are irreversible) and its effectivity upon very moderate increments of temperature.

Methods

Materials. 3,4-ethylenedioxythiophene (EDOT) and acetonitrile were purchased from Aldrich and used as received. Anhydrous $LiClO_4$, analytical from Aldrich, analytical reagent grade, was stored in an oven at 80 ºC before use in the electrochemical trials.

Preparation of PEDOT films. All systems studied in this work were obtained using a PGSTAT101 AUTOLAB potenciostat-galvanostat connected to a PC computer controlled through the NOVA 1.6 software, using a three-electrode one-compartment cell under nitrogen atmosphere at 25 ºC.

According to our previous studies, (Ocampo *et al*, 2006; Estrany *et al*, 2011, and Aradilla *et al*, 2012) PEDOT films in organic and aqueous environments were prepared by chronoamperometry (CA) under a constant potential of 1.40 and 1.10 V, respectively. The synthesis was carried out using a three-electrode one-compartment cell under nitrogen atmosphere (99.995% in purity) at 25 ºC. The cell was filled with 50 mL of a 10 mM monomer solution in acetonitrile or distilled water containing 0.1 M LiClO4 as supporting electrolyte. Steel AISI 316 sheets of 4 cm^2 area were employed as working and counter electrodes. The reference electrode was an Ag|AgCl electrode containing a KCl saturated aqueous solution (E^0 = 0.222 V vs. standard hydrogen electrode at 25 ºC), which was connected to the working compartment through a salt bridge containing the electrolyte solution.

Conductivity measurements. The electrical resistance of PEDOT was measured by connecting two wires to an ohmmeter, with their ends being pressed onto two lines of silver that defined the current path in the film (Figure 1). The film receives the heat dissipated by Joule effect resistance and modulates the intensity of the current flowing through it, which comes from a DC voltage source. As a result, the temperature of the film is controlled enabling gradual and continuous heating and cooling processes. In this work the heating rate was 1 ºC/min while cooling rate was 0.5 ºC/min. The measured resistance was used to determine the conductivity of the film:

$$\sigma = \frac{1}{R}\frac{L}{\ell} \qquad (1)$$

where R is the electrical resistance, L is the current path between the marks of silver, and l is the thickness of the film.

Thickness. Thickness of the films was determined by determining the current productivity through the mass-charge ratio and, subsequently, the mass of polymer deposited in the electrode. This procedure was detailed in a previous work (Estrany et al, 2007).

Atomic force microscopy (AFM). Topographic AFM images were obtained with a Molecular Imaging PicoSPM using a NanoScope IV controller under environmental conditions. The tapping mode AFM was operated at constant deflection. The row scanning frequency was set to 1 Hz. AFM measurements were performed on various parts of the films, which produced reproducible images similar to those displayed in this work. The scan window sizes used in this work were 5 × 5 μm^2. The root mean square roughness (Rq), which is the average height deviation taken from the mean data plane, the average roughness (Ra), which is the arithmetic average of the absolute values of the collected roughness data point, and the maximum roughness height (R_{max}), which is the maximum peak to lowest valley vertical distance within a single sample length, were determined using the statistical application of the NanoScope Analysis software.

	ℓ (μm)	Rq (nm)	Ra (nm)	Rmax (nm)	σ (S/cm)
	Before thermal treatment				
Acetonitrile	4.52±0.2	296±14	241±12	1581±96	109±8
Water	2.01±0.1	163±11	128±11	1007±68	1.1±0.5
	After heating-cooling cycle				
Acetonitrile	-	205±9	168±8	1336±47	196±6
Water	-	240±6	202±10	1366±28	9.5±1.3

Table 1. Thickness (ℓ), root mean square roughness (Rq), average roughness (Ra), maximum roughness (Rmax) and electrical conductivity (σ) of PEDOT prepared in acetonitrile and aqueous solutions before and after the thermal treatment.

Scanning electron microscopy (SEM). SEM studies were performed to examine the surface morphology of PEDOT before and after thermal treatment. Dried samples were placed in a Focussed Ion Beam Zeis Neon 40 scanning electron microscope operating at 3 kV, equipped with an EDX spectroscopy system.

X-ray diffraction (XRD). XRD spectra were recorded using a Bruker D8 Advance model to 40 kV and 40 mA (λ = 1.5406 Å). The XRD patterns were taken at ambient laboratory temperature using 10 s/angular step (1 angular step = 0.02°).

Thermal analysis. Calorimetric data were obtained with a TA Instruments Q100 series equipped with a refrigerated cooling system (RCS) operating at temperatures from -90 °C to 550 °C. Experiments were conducted under a flow of dry nitrogen with a sample weight of approximately 2 mg, calibration being performed with indium.

Results and discussion

Characterization of the films before thermal treatment

Thickness of the PEDOT films prepared in acetonitrile and water, which was determined by electrochemical procedures, is ℓ= 2.02 and 0.46 μm, respectively. Obviously, this difference is not only due to the solvent, but also to the different potentials used in the anodic polymeric process. On the other hand, the topography and morphology of the films were studied by AFM and SEM, respectively. Films prepared in acetonitrile show large and broad blocks of aggregated polymer chains emerging from relatively flat and narrow regions (Figure 2a). The Rq and Ra values determined for such films are lower than 300 nm while Rmax reaches a value close to 1.5 μ m (Table 1). This topography is fully consistent with the main morphological features observed by SEM. Thus, the micrograph displayed in Figure 2b shows micrometric clusters formed through the aggregation of fiber-like thin sticks, which in turn results from the aggrupation of linear polymer molecules (*i.e.* PEDOT molecules are exclusively formed by α-α linkages). However, the most important feature revealed by SEM is the notable porosity of these films. Furthermore, such porosity is highly heterogeneous since clusters are separated by relatively wide and tortuous pores of submicrometric dimensions while the sticks contained in each cluster are separated by very small nanometric pores.

The substitution of acetonitrile by water drastically affects the thickness of the film, which reduces more than a half (Table 1). The topography and morphology of films prepared in water are completely different from that of films prepared in the organic environment. As is reflected in the AFM and SEM images displayed in Figures 3a and 3b, respectively, the surface of PEDOT films obtained in an aqueous solution can be described as a homogeneous and compact distribution of small clusters. This provokes a significant reduction of the roughness, which decreases by about 45% with respect to films generated in acetonitrile (Table 1), and the porosity. Thus, both wide and narrow pores identified in the inter-cluster and inter-stick regions, respectively, of films prepared in acetonitrile practically disappear for the films produced in aqueous solution.

In addition to the structural properties, the generation medium also affects the conductivity of PEDOT. In spite of the same dopant was used for the two electrochemical media, films produced in acetonitrile are two orders of magnitude higher than that of films obtained in an aqueous environment (Table 1). This observation is fully consistent with the structural features discussed above since charge movement becomes more difficult with increasing compactness.

Thermal treatment of PEDOT films

Pristine PEDOT films were progressively heated from room temperature (25 °C) to 70 °C at a rate of 1 °C/min, the conductivity being registered at each step. After reaching the highest temperature, films were subsequently cooled at a rate of 0.5 °C/min. The conductivity was automatically registered at every step as indicated in the Methods section (Figure 1). As it was expected, conductivity increases with the temperature within the examined interval of temperatures, even though the two systems showed different behaviours (Figure 4). Films prepared in acetronitrile experienced a progressive and continuous increment of the temperature, reaching a value of 179 S/cm at 70 °C. In contrast, conductivity of the film prepared in water increased from 1.1 S/cm at 25 °C to 8 S/cm at 50 °C, stabilizing around such value until the final temperature was reached. The fact that the two films behave different is consistent with their different morphology and topography (see next subsection).

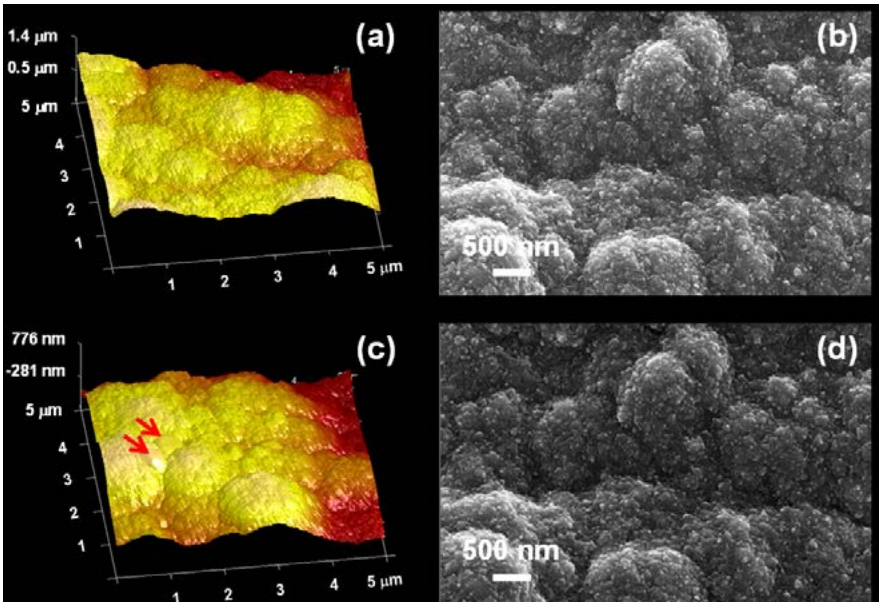

Figure 3. 3D AFM and SEM micrographs for PEDOT prepared in water: (a,b) pristine samples; and (c,d) samples subjected to heating-cooling treatment.

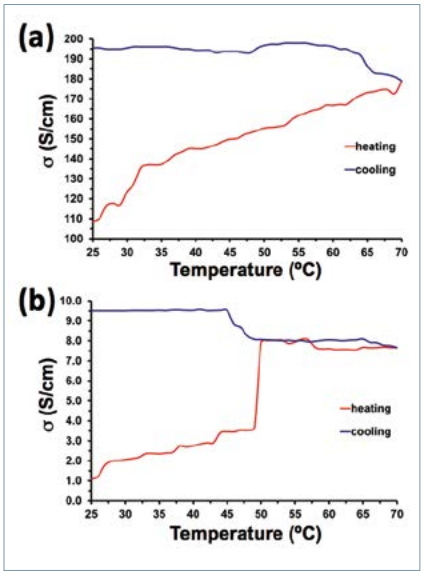

Figure 4. Variation of the conductivity (σ) during the progressive and continuous heating (1 °C/min) and subsequent cooling (0.5 °C/min) of PEDOT films prepared in (a) acetonitrile and (b) water.

The most interesting results refer to the variation of the conductivity upon cooling from 70 ºC to 25 ºC. Figure 4 reflects that conductivity still increases a little bit with respect to the values reached at the end of the heating process. Accordingly, the enhanced electric behaviour is irreversible, which evidences that progressive and slow heating of PEDOT films is a very efficient treatment to improve the electric performance of PEDOT. Accordingly, electrical conductivity at 25 ºC measured for films prepared in acetonitrile and water after the heating-cooling process is 196 and 9.5 S/cm. This represents an increment of 80% and 864% for PEDOT films prepared in acetonitrile and water, respectively. It should also be mentioned that this effect is stable, the conductivities measured after the heating-cooling cycle being retained after several days. Graphics displayed in Figure 4 are fully reproducible, even though we found that thermal stress provokes mechanical breaking of films with thickness of $\ell \leq 200$ nm. Therefore, the proposed thermal treatment is not applicable to films of nanometric thickness.

On the other hand, the drastic change observed at 50 ºC in the heating profile for the films prepared in water (Figure 4b) could also be due to a partial melting of PEDOT crystals. Indeed, an important discontinuity is observed in the cooling profile at a slightly lower temperature, which suggests a recrystallization process. This feature is consistent with the crystallinity of PEDOT samples prepared in water, which has been found to considerably important (see below).

According to the variable range hopping (VRH) mechanism (Mott, 1969), charge transport is described as:

$$\sigma = \sigma_0 \exp\left(\frac{-T_0}{T}\right)^{\frac{1}{1+n}} \qquad (2)$$

where σ_0 and T0 are the pre-exponential and exponential factors, respectively, and n is the hopping space dimensionality. The value of the latter can be $n = 1, 2$, or 3, which corresponds to a one-, two- and three-dimensional systems, respectively. Figure 5 indicates that during the heating process the charge transport in PEDOT films is dominated by the 3D VRH mechanism ($n = 3$). Thus, there is a linear relation between the Ln σ against $T^{-1/4}$, corroborating that the conductivity is represented by:

$$\sigma = \sigma_0 \exp\left(\frac{-T_0}{T}\right)^{\frac{1}{4}} \qquad (3)$$

In case the film is produced in water, the 3D VRH mechanism is consistent up to T= 50 ºC only, suggesting drastic structural changes after reach such temperature.

The 3D mechanism is completely lost in the cooling process for the two films, as it is evidenced by the poor regression coefficients displayed in Figure 5 (analyses of different fragments of the profile led to even poorer correlation coefficients). Moreover, detailed analyses indicated that the cooling profile, completed or the interval obtained for T < 50 ºC, does not fit well to the 1D nor the 2D VRH equations (*i.e.* $n = 1$ and $n = 2$ in Eqn 2), regression coefficients lower than 0.6 being obtained in all cases (not shown). This suggests that the heating process provoked important structural changes and, as a consequence, the charge transfer change from 3D VRH to a mixture of mechanisms. Understanding of this phenomenon is provided in the structural analysis of the next sub-section.

Structural changes provoked by thermal treatment

Figures 2c and 2d show 3D AFM and SEM micrographs, respectively, recorded for PEDOT generated in acetonitrile after the heating-cooling cycle while Table 1 displays the effect of the thermal treatment in the roughness. Although surface morphologies before and after thermal treatment are apparently very similar, the surface

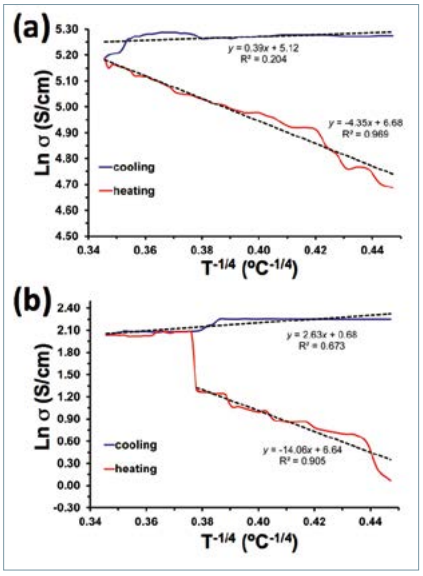

Figure 5. Temperature dependence of the conductivity for PEDOT prepared in (a) acetonitrile and (b) water during the heating and cooling processes. Dashed straight lines are fits to Equation (3).

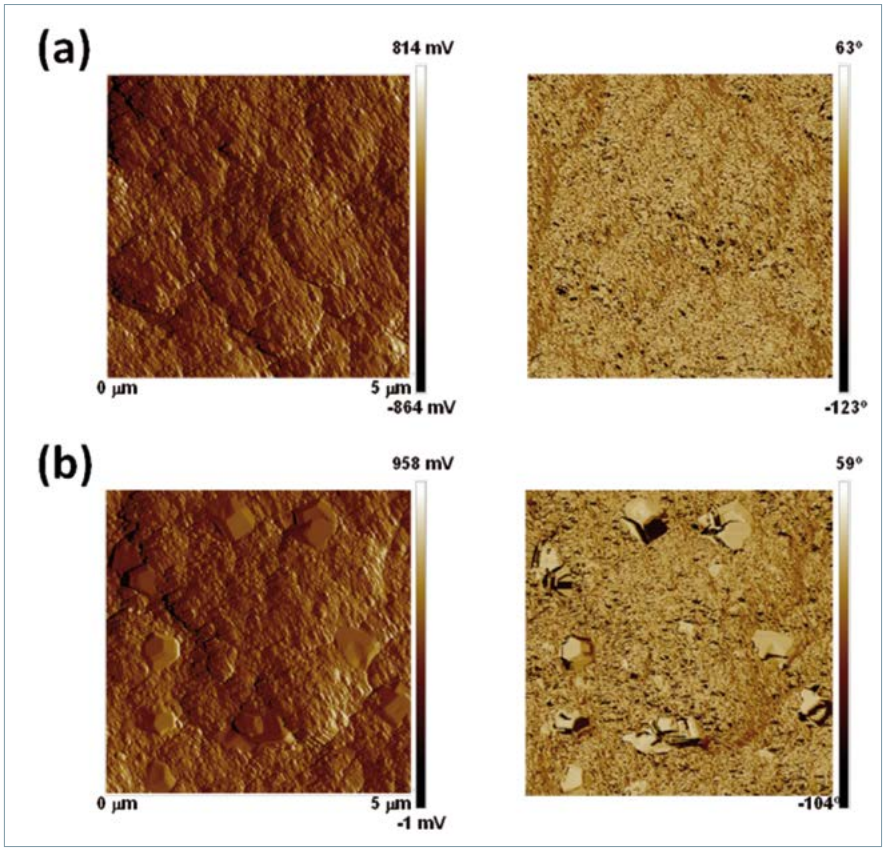

Figure 6. AFM micrographs PEDOT films generated in water (a) before and (b) after the heating-cooling cycle: 2D height (left) and phase (right) images.

porosity is lower for the treated film. Thus, large and tortuous inter-cluster pores remain but small inter-stick pores are significantly shorter suggesting local reorganizations of the sticks that lead to more compact structures. Topographic AFM images evidences that submicrometric aggregates observed before heating are smaller and more abundant after the thermal cycle. This provokes a reduction in the roughness of around 30%. 2D topography and phase AFM images did not provide any additional information (not shown). According to these observations, the increment of the conductivity provoked by the thermal treatment (*i.e.* x1.8) must be ascribed to local redistributions of the polymer chains.

A completely different situation is detected for the PEDOT films prepared in water. Although SEM micrographs recorded for treated samples show a compact morphology like that obtained for the pristine film (Figure 3d), 3D AFM images evidence significant changes in the topography (Figure 3c). The most significant one corresponds to the apparition of agglomerates with polyhedral shape (marked with arrows in Figure 3c). Thus, these agglomerates show faces and edges embedded in small globular clusters similar to those already observed in the non-treated films. The apparition of these polyhedral aggregates provokes an increment in the roughness of around 20%, even though R_{max} remains practically at the same value. This can be interpreted in two different ways: (1) as a reorganization of polymer chains located at the deep valleys, which now emerge as regular clusters (*crystallization mechanism*); or (2) as a redistribution of the small clusters detected in pristine films to form bigger and well-defined agglomerates at the surface (*percolative mechanism*). It should be noted that the latter mechanism is also consistent with a redistribution of the crystals through partial melting of the crystals at 50 ºC during the heating and subsequent recrystallization process at 48 ºC during the cooling.

2D Height and phase AFM images of the films obtained in water before and after the treatment, which are compared in Figure 6, provide more information about the above mentioned features. As it can be seen, well-defined polyhedral aggregates, which are completely absent in the pristine films (Figure 6a, left), appear after thermal treatment (Figure 6b, left). Furthermore, the fact that the contrast in the phase image after thermal treatment (Figure 6b, right) is the same that in the image before the heating-cooling cycle (Figure 6a, right) corroborates that polyhedral aggregates are made of PEDOT, allowing us to discard the possible crystallization of electrolyte salts at the surface.

As mentioned above, the overall of the results obtained in this work suggest that the applied thermal treatment provokes a local reorganization of the polymer chains to form more ordered domains or the local redistribution of polymer clusters to form compact agglomerates. The possible existence of the crystallization mechanism was ascertained by recording the XRD pattern of samples before and after the thermal treatment. Results for the samples prepared in acetonitrile, which are displayed in Figure 7a, show two weak peaks centred at 2θ= 6.8º (broad) and 29.6º (sharp). The intensity of the peak at 2θ= 29.6º, which was identified as the stacking distance (i.e. ~3.4 Å) between polymer chains in crystalline doped PEDOT (Aasmundtveit, 1999), in-

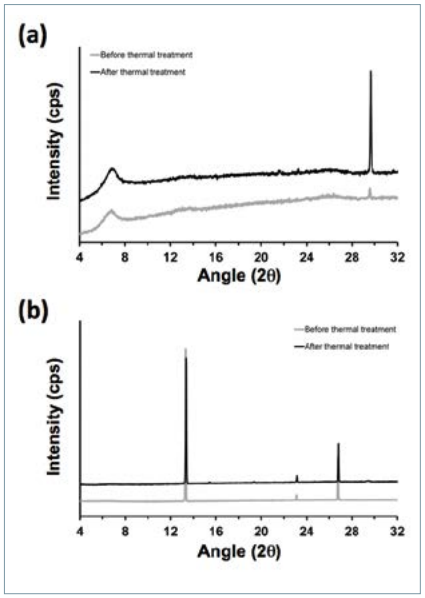

Figure 7. XRD patters of PEDOT films generated in (a) acetonitrile and (b) water before and (b) after the heating-cooling cycle.

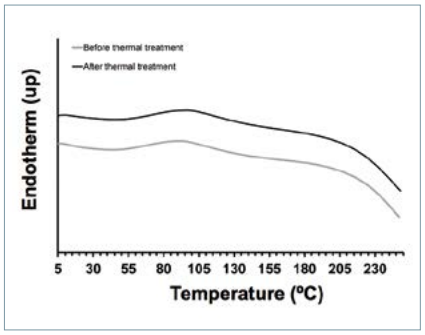

Figure 8. DSC curves of PEDOT generated in water before and after the heating-cooling cycle.

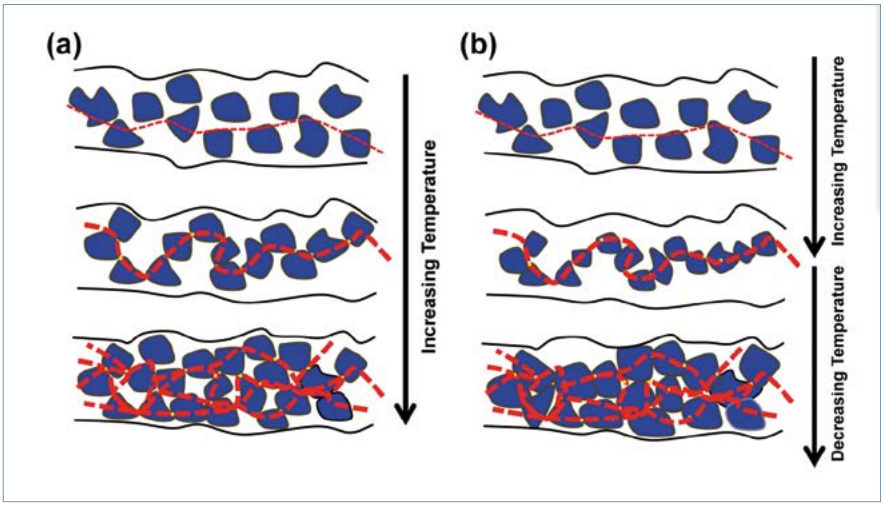

Figure 9. Schematic representation of the re-organized experienced by PEDOT clusters (blue particles) in films prepared in water. Two possible microscopic of the percolative mechanism (see text) are depicted in (a) and (b).

creases significantly after thermal treatment with respect to the intensity of the peak at 2θ= 6.8º. This feature indicates that the thermal treatment promotes the crystallization of the polymer chains, which is fully consistent with the crystallization mechanism. According to this, the increase of temperature promoted the reorganization of the initial compact structures favouring the formation of some microcrystals in which random orientation of the chains tends to disappear. These stable microcrystals, which were detected by AFM at the surface of thermally treated films as ordered submicrometric aggregates, remained after completing the cooling process. As the thermal stress induced by the moderate temperature increment used in this work was not enough to achieve a complete re-organization of the polymer chains, regions with different degrees of organization would coexist in the film, explaining the mixture of VRH charge transport mechanisms detected during the cooling process (Figure 5).

The behaviour of the XRD profiles obtained for samples prepared in water before and after thermal treatment (Figure 7b) is the opposite of that discussed above for PEDOT obtained in acetonitrile. Samples obtained in water present three sharp diffraction peaks at 2θ= 13.3º (very intense), 23.1º (weak), and 26.7º (intense). As it can be seen, the relative intensity of the peaks does not undergo significant changes upon heating, indicating similar crystallinities for the two samples. This result is corroborated by DSC profiles displayed in Figure 8, which were registered for PEDOT samples before and after thermal treatment. As it can be seen, the two profiles show an endothermic process at ~85 ºC with very similar enthalpies that has been attributed to the melting of the crystalline phase (Meng, 2003).

According to these features, the significant and irreversible increment of the electrical conductivity observed after the heating-cooling cycle has been attributed to the percolative mechanism, which can be microscopically interpreted in two different ways as is schematically illustrated in Figure 9. In the first in interpretation (Figure 9a), as long as the temperature increases slowly, the clusters formed during the preparation process stack forming compact and regular polyhedral aggregates. When this percolation threshold occurs, the number of interconnections and long-range connectivity improve, thus leading to enhanced electrical conductivity. In the second interpretation (Figure 9b), it is similar to the previous one but including a melting-recrystallization process. Thus, the formation of inter-connection upon heating is accompanied by the partial melting of the crystals, which occurs at 50 ºC. Subsequently, recrystallization occurs during cooling, increasing the size of these crystals and facilitating the connectivity.

Conclusions

A simple but very efficient thermal treatment is proposed to improve irreversibly the electrical properties of PEDOT films prepared in organic and, especially, aqueous solution. This treatment consists of a heating-cooling cycle in which the temperature (1 ºC/min) is slowly increased from 25 ºC to only 70 ºC and, subsequently, cooled at room temperature very slowly (0.5 ºC/min). After this treatment, the electrical conductivity of films prepared in acetonitrile and aqueous environment increases by a factor of x1.8 and x8.6, respectively. AFM, SEM, XRD and DSC studies show that the heating-cooling cycle provokes local structural

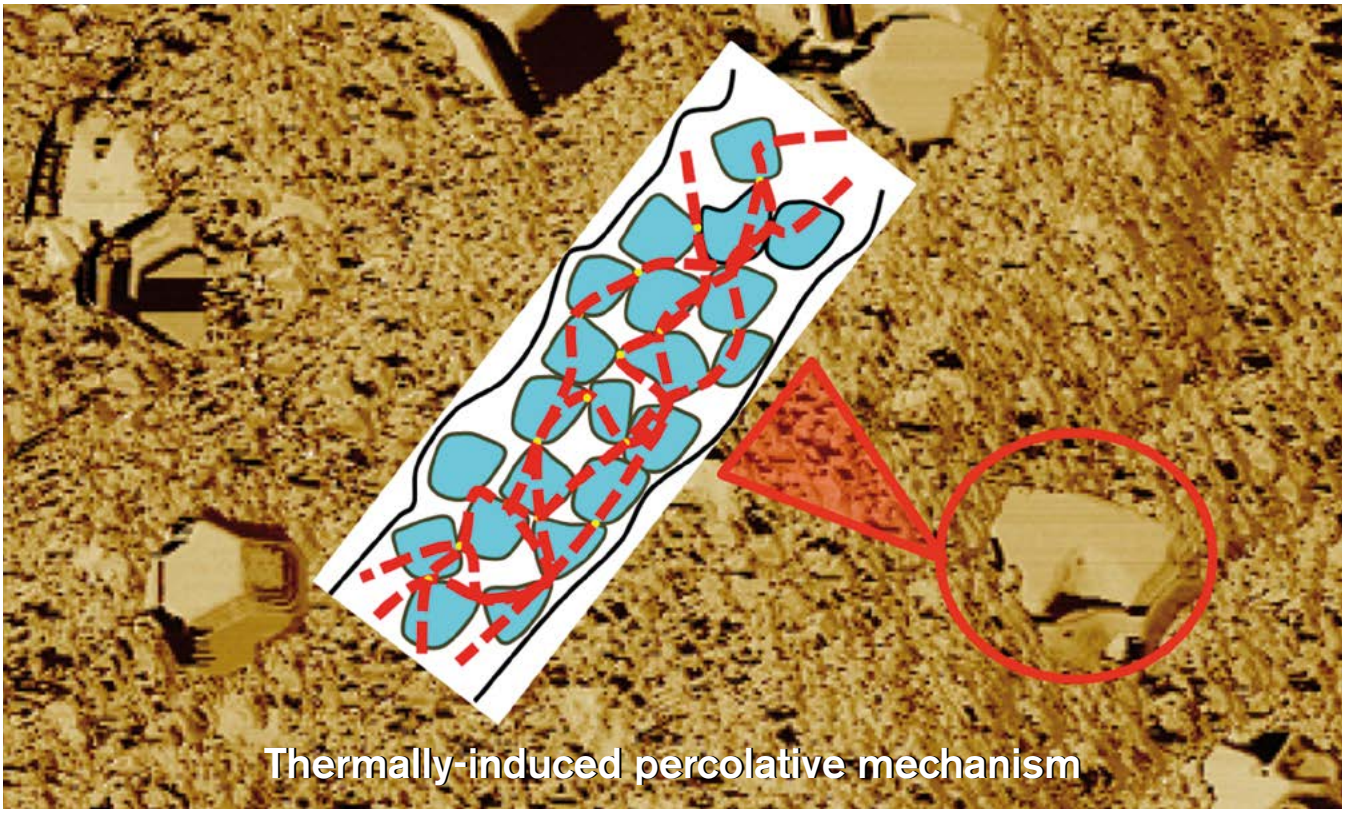

Graphical Abstract.

re-arrangements, which are more or less drastic depending on the porosity of the sample. In the case of films prepared in aqueous solution, the thermal treatment promotes a percolative mechanism through the formation of sub-micrometric aggregates that can be accompanied by melting-recrystallization processes. Interconnections in these aggregates, which are clearly detected in the surface of samples as polyhedral particles, result in a significant enhancement of the electrical conductivity. In these samples the thermally-induced transition accompanied by the corresponding irreversible increment of conductivity occurs at only 50 ºC.

Acknowledgements

This work was MICINN-FEDER funds (MAT2012-34498 and MAT2012-3625) and by the Generalitat de Catalunya (XRQTC). The authors also thank the Brazilian Government agencies CNPq and CAPES (process BEX 457 13736124) for the scholarship of R.S Peres.

References

Aasmundtveit KE, Samuelsent EJ, Pettersson LAA, Inganas O, Johansson T and Feidenhans R (1999). *Synth. Met.* 101: 561-564.

Aradilla D, Azambuja D, Estrany F, Casas MT, Ferreira CA and Alemán C (2012). *J. Mater. Chem.* 22: 13110-13122.

Aradilla D, Estrany F, Casellas F, Iribarren JI and Alemán C (2014). *Org. Electron.* 15: 40-46.

Atanasov SE, Losego MD, Gong B, Sachet E, Maria JP, Williams PS and Parsons GN (2014). *Chem. Mater.* 26: 3471-3478.

Bubnova O, Khan ZU, Malti A, Braun S, Fahlman M, Berggren M and Crispin X (2011). *Nature Mater.* 10: 429-433.

Castagnola V, Bayon C, Descamps E and Bergaud C (2014). *Synth. Met.* 189: 7-16.

Culebras M, Gómez CM and Cantarero A (2014). *J. Mater. Chem. A.* 2: 10109-10115.

Dayal S, Reese M O, Ferguson A J, Ginley D S, Rumbles G and Kopidakis N (2010). *Adv. Funct. Mater.* 20: 2629-2635.

Estrany F, Alemán C, Armelin E and Casanovas J (2011). *Técnica Industrial.* 291: 24-33.

Estrany F, Aradilla D, Oliver R and Alemán C (2007). *Eur. Polym. J.* 43: 1876-1882.

Groenendaal LB, Jonas F, Freitag D, Pielartzik H and Reynolds JR (2000). *Adv. Mater.* 12: 481-494.

Hoppe H and Sariciftci NS (2006). *J. Mater. Chem.* 16: 45-61.

Jang K S, Eom Y S, Lee T W, Kim D O, Oh Y S, Jung H C and Nam J D (2009). *Appl. Mater. Interfaces*, 1: 1567-1571.

Jang K S, Kim D O, Hee J H, Hong S C, Lee T W, Lee Y and Nam J D (2010). *Org. Electron.* 11: 1668-1675.

Joo J, Park SH, Seo DS, Lee SJ, Kim HS, Ryu KW, Lee TJ, Seo SH and Lee CL (2005). *Adv. Funct. Mater.* 15: 1465-1470.

Kim Y, Cook S, Tuladhar S M, Choulis S A, Nelson J, Durrant J R, Bradley D D C, Giles M, McCulloch I, Ha C S and Ree M (2006). *Nature Mater.* 5: 197-203.

Kirchmeyer S and Reuter K (2005). *J. Mater. Chem.* 15: 2077-2088.

Koh JK, Kim J, Kim B, Kim JH and Kim E (2011). *Adv. Mater.* 23: 1641-1646.

Kumar A, Welsh DM, Morvant MC, Piroux F, Abboud KA and Reynolds JR, Chem. Mater. 1998, 10, 896-902.

Lee SH, Park H, Kim S, Son W, Cheong W and Kim JH (2014). J. Mater. Chem. A. 2: 7288-7294.

Luo J, Billep D, Waechtler T, Otto T, Toader M, Gordan O, Sheremet E, Martin J, Hietschold M, Zahn DRT and Gessner T (2013). J. Mater. Chem. A. 1: 7576-7583.

Meng H, Perepichka D, Bendikow M, Wudl F, Pan GZ, Yu W, Dong W and Brown S (2003). J. Am. Chem. Soc.,125: 15151-15162.

Mott, NF (1969). Philos. Mag. 19: 835-852.

Nardes AM, Ferguson AJ, Whitaker JB, Larson BW, Larsen RE, Maturová K, Graf PA, Boltalina OV, Strauss SH and Kopikadis N (2012). *Adv. Funct. Mater.* 22: 4115-4127.

Nardes AM, Janssen RAJ and Kemerink M (2008). *Adv. Funct. Mater.* 18: 865-871.

Nielsen C B and McCulloch I (2013). *Prog. Polym. Sci.* 38: 2053-2069.

Ocampo C, Oliver R, Armelin E, Alemán C and Estrany F (2006). *J. Polym. Res.* 13: 193-200.

Pettersson L, Johansson T, Carlsson F, Arwin H and Inganas O (1999). *Synth. Met.* 1999, 101: 198-199.

Schwartz BJ (2003). *Ann. Rev. Phys. Chem.* 54: 141-172.

Tada K (2013). *Sol. Energ. Mat. Sol. C*, 108: 82-86.

Wilson P Lekaku C and Watts J (2013). *Org. Electr.* 14: 3277-3285.

Winther-Jensen B, Winther-Jensen O, Forsyth M and MacFarlane DR (2008). *Science*, 321: 671-674.

Wu D, Zhag J, Dong W, Chen H, Huang X, Sun B and Chen L (2013). *Synth. Met.* 176: 86-91.

Xia Y and Ouyang J (2010). *Appl. Mater. Interfaces.* 2: 474-483.

Xuan Y, Sandberg M, Berggren M and Crispin X (2012). *Org. Electron.* 13: 632-637.